Kinetics of Adhesion of IgE-Sensitized Rat Basophilic Leukemia Cells to Surface-Immobilized Antigen in Couette Flow

David G. Swift,* Richard G. Posner,# and Daniel A. Hammer*
*Department of Chemical Engineering, University of Pennsylvania, Philadelphia, Pennsylvania 19104, and #Department of Chemistry, Northern Arizona University, Flagstaff, Arizona 86011-5698 USA

ABSTRACT Antigen-antibody systems provide the flexibility of varying the kinetics and affinity of molecular interaction and studying the resulting effect on adhesion. In a parallel-plate flow chamber, we measured the extent and rate of adhesion of rat basophilic leukemia cells preincubated with anti-dinitrophenyl IgE clones SPE-7 or H1 26.82 to dinitrophenyl-coated polyacrylamide gel substrates in a linear shear field. Both of these IgEs bind dinitrophenyl, but H1 26.82 has a 10-fold greater on rate and a 30-fold greater affinity. Adhesion was found to be binary; cells either arrested irreversibly or continued at their unencumbered hydrodynamic velocity. Under identical conditions, more adhesion was seen with the higher affinity (higher on rate) IgE clone. At some shear rates, adhesion was robust with H1 26.82, but negligible with SPE-7. Reduction in receptor number or ligand density reduced the maximum level of adhesion seen at any shear rate, but did not decrease the shear rate at which adhesion was first observed. The spatial pattern of adhesion for both IgE clones is well represented by the first-order kinetic rate constant k_{ad}, and we have determined how k_{ad} depends on ligand and receptor densities and shear rate. The rate constant k_{ad} found with H1 26.82 was approximately fivefold greater than with SPE-7. The dependence of k_{ad} on site density and shear rate for SPE-7 is complex: k_{ad} increases linearly with antigen site density at low to moderate shear rates, but is insensitive to site density at high shear. k_{ad} increases with shear rate at low site density but decreases with shear at high site density. With H1 26.82, the functional dependence of k_{ad} with shear rate was similar. Although these data are consistent with the hypothesis that we have sampled both transport and reaction-limited adhesion regimes, they point out deficiencies in current theories describing cell attachment under flow.

INTRODUCTION

The high-affinity, high-specificity binding of cell-bound macromolecular receptors to surface coreceptors, or ligands, is of considerable importance in the fields of medicine and biotechnology. The receptor-mediated (specific) adhesion of cells to surfaces is a vital physiological process. Cell adhesion is a key event in many normal physiological processes, including the inflammatory response (Atherton and Born, 1972) and lymphocyte homing (Springer, 1990). In particular, the adhesion of neutrophil to the endothelium in vivo depends on receptor-ligand recognition (Dore et al., 1993; Ley et al., 1993; Springer, 1990). Normal lymphocyte homing to secondary lymphoid tissues in the immune system also depends on the recognition of cell surface receptors (Kansas, 1996). Cancer cells rely on this process during metastasis (Pauli et al., 1990).

The adhesion of cells to surfaces under conditions of flow represents a balance between physical and chemical forces (Hammer and Apte, 1992). The chemical bonding force delivered by the receptor-ligand pair balances the hydrodynamic forces on the cell. This chemical bonding force is derived from the numbers and strength of adhesive linkages between cell and surface, which result from the properties of the adhesion molecules. Different functional properties of molecules give rise to different dynamic states of adhesion, such as rolling or firm adhesion (Chang, 1997; Hammer and Apte, 1992). Under hydrodynamic flow, different types of adhesion have been observed: firm adhesion, transient tethering, and rolling at reduced velocity (Alon et al., 1995; Lawrence and Springer, 1993; Tempelman and Hammer, 1994).

In addition, the magnitude of adhesion (extent of adhesion or rate of rolling) is also dependent on the receptor and ligand surface site densities (Brunk and Hammer, 1997; Tempelman and Hammer, 1994; Hammer and Apte, 1992).

Understanding how adhesion is controlled at the molecular level is important in developing technologies. The high specificity of receptor-ligand binding provides an extremely sensitive means of cell manipulation, cell selection, and cell-based diagnostics. Provided we can characterize the properties of the molecules that mediate adhesion and relate these to the magnitude and state of adhesion, we can intelligently design devices that employ cell adhesion in medicinal and biotechnological applications. Thus exploitation of specific cellular adhesion would be aided by a fundamental understanding of how adhesion is controlled at the molecular level.

In this paper we present results for the binding of cells coated with antibodies to surface-immobilized antigens under linear shear flow. Antigen-antibody systems provide robust flexibility for manipulating molecular properties, because so many antigen-antibody pairs of different affinity and kinetics are available. We use rat basophilic leukemia

Received for publication 26 March 1998 and in final form 31 July 1998.
Address reprint requests to Dr. Daniel A. Hammer, Department of Chemical Engineering, University of Pennsylvania, 311A Towne Bldg., 220 S. 33rd St., Philadelphia, PA 19104. Tel.: 215-573-6761; Fax: 215-573-2093; E-mail: Hammer@seas.upenn.edu.

0006-3495/98/11/2597/15 $2.00

(RBL) cells as a model system for measuring adhesion (Tempelman and Hammer, 1994). With this system, we can systematically vary receptor-ligand binding kinetics and affinity (through selection of different antigen-IgE pairs), site densities, and fluid shear stresses. The chemistry is shown in Fig. 1. RBL cells are coated with murine monoclonal anti-2,4-dinitrophenyl (DNP) IgE, and the surface is coated with 2,4-DNP-ϵ-lysine. We have extended the work of Tempelman and Hammer (1994) by measuring adhesion for two different IgE clones, SPE-7 and H1 26.82, which have different on rates and affinities. RBL cells bind with high affinity to the Fc portion of murine IgE molecules via the cell-surface Fc_ϵ receptor ($K_A = 10^{10}$ M^{-1}) (Metzger et al., 1986). Using this system only with the H1 26.82 anti-DNP IgE clone, Tempelman and Hammer observed that cell binding was binary, sensitive to shear, and strongly dependent on the number of anti-DNP binding sites (Tempelman and Hammer, 1994). By comparing the adhesion mediated by either antigen-antibody or antibody-receptor binding, they also observed that the forward binding rate appears more important than thermodynamic affinity for cell attachment, with the extent of attachment increasing with forward binding rate. In this paper we compare adhesion mediated by H1 26.82 to that mediated by a different antibody-antigen pair (SPE-7/DNP) of different kinetics and affinity, with our primary focus on the SPE-7/DNP pair.

An additional question addressed in this paper is why different receptor-ligand pairs give rise to different dynamic states of adhesion. Selectin adhesion molecules mediate rolling. Our laboratory has shown that rolling can be recreated using cell-free systems in which carbohydrate-coated spheres roll over selectin substrates (Brunk et al., 1997). Alon and co-workers have postulated that rolling results from the fast on rates, fast off rates, and unique mechanical properties of selectin-carbohydrate bonds (Alon et al., 1995). By using antigen-antibody pairs with lower affinities and faster off rates, such as we use in this paper (indeed, systems with kinetic rates close to the values cited for selectin-carbohydrate interactions), we can test whether rolling is a result of fast receptor-ligand kinetics.

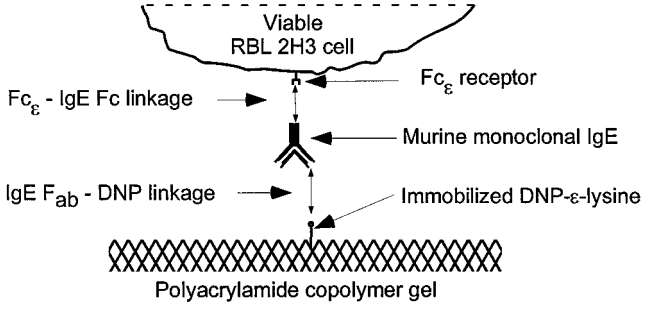

FIGURE 1 A schematic diagram showing the chemistry used in RBL cell adhesion experiments. RBL cells (5×10^6/ml) are incubated with a 50 nM mixture of anti-DNP IgE and the neutral antibody anti-DNS to fill 0–100% of 2×10^5 cell-surface Fc_ϵ receptors per cell with anti-DNP antibody. Binding is mediated by Fab-antigen binding as shown.

In this paper, we focus largely on a new IgE clone, SPE-7, which has a lower binding affinity for DNP than H1 26.82. We determine if SPE-7 mediates a dynamic state of adhesion different from that of H1 26.82, and differences in the sensitivity of adhesion to shear rate or ligand density. Furthermore, in this paper we define a rate constant for adhesion and measure how it depends on receptor and ligand affinities, rates, and densities, and shear rate. With this parameter, we concisely represent the rate of cell-substrate binding in adhesion assays, allowing us to readily compare cell-binding rates for a variety of conditions.

In this work we measured the adhesion of RBL cells sensitized with SPE-7 and H1 26.82 IgE to DNP-coated substrates under wall shear rates in the range of 20–140 1/s. We observed only binary binding (firm adhesion) with both of these chemistries. We could manipulate the extent of cell attachment from complete to negative control by varying shear rate in this range. The extent of adhesion was also found to depend strongly on receptor and ligand surface densities under most conditions. The adhesion rate constant was calculated from the spatial pattern of cell attachment. This parameter was found to depend nearly linearly on receptor and ligand site densities, but to exhibit a complex dependence on the wall shear rate. We believe that this study represents the first attempt to relate the rate constant for cell adhesion to wall shear rate, receptor, and ligand site densities, and receptor-ligand binding kinetics.

MATERIALS AND METHODS

Flow cytometric equilibrium binding assays

Cytometric binding assays were performed on a Becton-Dickinson FACScan flow cytometer interfaced with a Macintosh computer running Cell Quest software. A suspension of RBL-2H3 cells in freshly filtered buffered salt solution (135 mM NaCl, 5 mM KCl, 1 mM $MgCl_2$, 1.8 mM $CaCl_2$, 5.6 mM glucose, 0.1% gelatin, 20 mM HEPES) was equilibrated in the presence of various concentrations of DNP-lysine for at least 20 min at room temperature. The number of Fab arms occupied by DNP groups was determined by measuring the decrease in fluorescein isothiocyanate (FITC) fluorescence (FL1) that occurs when DNP binds to FITC-labeled anti-DNP IgE (Erickson et al., 1986).

The equilibrium binding constant was determined as previously described (Goldstein et al., 1989). The concentration of bound ligand $L^* = KR_TL/(1 + KL)$, where $L = L_T - L^*$ is the free ligand concentration, L_T is the total ligand concentration, and R_T is the total receptor site (Fab sites) concentration. Solving for L^*, we obtain

$$L^* = (1 + KL_T + KR_T - [(1 + KL_T + KR_T)^2 - 4K2R_TL_T]^{1/2})/2K$$

L^* is related to the relative fluorescence F, because binding leads to quenching. Thus $L^*/R_T = (F_H - F)/(F_H - F_L)$, where F_H is the fluorescence value when all receptor sites are empty and F_L is the fluorescence value when all receptor sites are occupied. To determine K, we fit the above equation to a titration curve, taking as free parameters K, F_H, and F_L. Fig. 2 illustrates this method for the SPE-7 IgE/DNP-ϵ-lysine pair.

Spectrofluorimetric binding assays

Kinetic binding experiments were performed on a SPEX fluoromax spectrofluorimeter and followed the procedure described by Erickson et al.

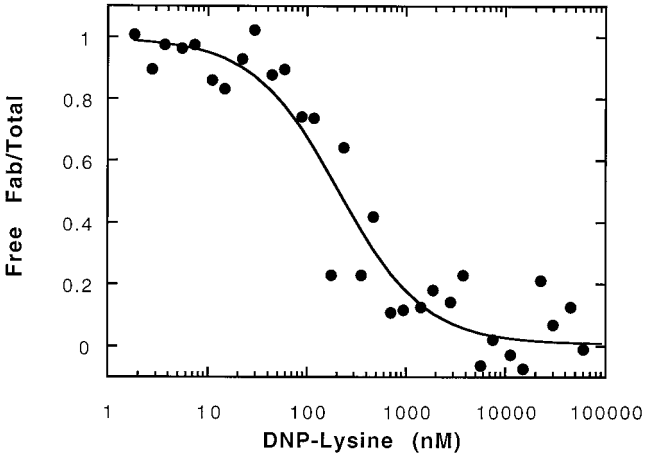

FIGURE 2 Equilibrium binding of DNP-lysine to SPE-7 FITC-IgE bound to receptors on RBL cells (10^6/ml) as measured by quenching of FITC-IgE fluorescence. Plotted is the fraction of free receptors as a function of the DNP-lysine concentration (●). The solid line was obtained from a nonlinear least-squares fit of the data (see Materials and Methods) and yielded an equilibrium constant $K_A = 4.8 \times 10^6\ M^{-1}$.

(1986, 1987, 1991). The quenching data were fit to a bimolecular scheme:

$$L + R \Leftrightarrow L^*$$

which yields the following differential equation:

$$dL^*/dt = k_{on}LR - k_{off}L^*$$

where $L^*/RT = (F_H - F)/(F_H - F_L)$, as described above.

Differential equations were solved numerically using the Common Los Alamos Mathematics and Statistics Library (CLAMS) subroutine DDRVB2. Parameter estimates were obtained using the CLAMS subroutine DNLS1, which is based on a finite-difference Levenberg-Marquardt algorithm for solving nonlinear least-squares problems. Fig. 3 illustrates this method for the SPE-7 IgE/DNP-ϵ-lysine pair.

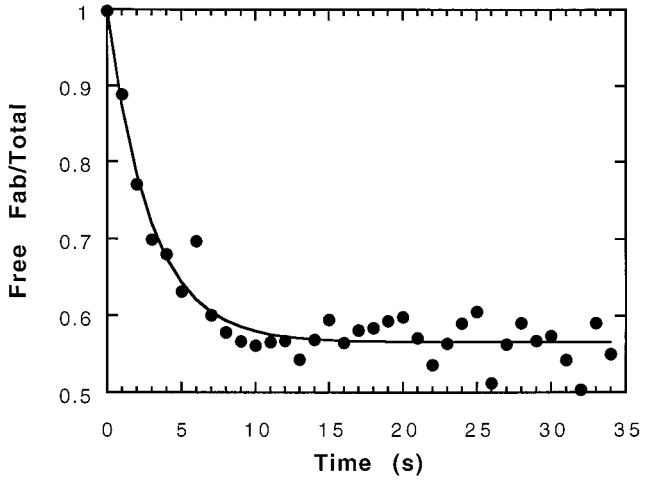

FIGURE 3 Determination of the rate constant for the binding of DNP-lysine to SPE-7 FITC-IgE in solution. Shown are typical quenching data and best fit of the equation that follows from a simple bimolecular scheme (see Materials and Methods). K_A is fixed at $4.8 \times 10^6\ M^{-1}$, $[Fab]_{bulk} = 5.0$ nM, and $[DNP\text{-}lys]_{tot} = 160$ nM. The best fit (*solid line*) obtained is $k_{on} = 9.35 \times 10^5\ M^{-1}\ s^{-1}$.

Antibody-sensitized cells

The RBL cell subline 2H3 (Barsumian et al., 1981) was a generous gift from Dr. Barbara Baird (Cornell University, Ithaca, NY). These cells were cultured and harvested as previously described for use between days 3 and 6 (Taurog et al., 1979). Harvested cells are spherical and vary in diameter from 12 to 17 μm (mean ~15 μm), as indicated by brightfield microscopy. Cells are highly microvilliated, with 3000 microvilli per cell (Oliver et al., 1988). Microvilli are 0.5 μm long, with a tip area of 0.01 μm^2 (Bongrand and Bell, 1984; Oliver et al., 1988). RBL cells possess on average 2×10^5 Fc_ϵ receptors per cell (Barsumian et al., 1981; Metzger et al., 1986).

Mouse monoclonal anti-DNP IgE from clone SPE-7 (Sigma, St. Louis, MO) was used as the DNP-binding antibody in the majority of trials. Mouse monoclonal anti-DNP from clone H1 26.82, a generous gift from Dr. Barbara Baird, was also used as a DNP-binding antibody. Mouse monoclonal anti-dansyl IgE from clone 2774 (PharMingen, San Diego, CA) was used as a neutral antibody that does not bind DNP. Cells (5×10^6/ml) were incubated for 1 h at 37°C in media containing 50 nM IgE. Flow cytometry analysis indicates saturation binding of FITC-IgE (clone SPE-7) under these conditions (data not shown). The anti-DNP/anti-dansyl IgE ratio was adjusted to fill between 0 and 100% of the cell surface Fc_ϵ receptors with anti-DNP (Weetal, 1992). In this way, we can adjust the total number of DNP-binding sites from 0 to 100% of the 4×10^5 DNP binding sites per cell (IgE is bivalent). After incubation with IgE, cells were centrifuged and resuspended in a modified Tyrode's buffer (125 mM NaCl, 5 mM KCl, 10 mM HEPES, 1 mM $MgCl_2$, 1.8 mM $CaCl_2$, 0.10% gelatin, and 5.6 mM glucose in deionized water at 1–2 $\times$ 10^6/ml and held at 37°C for use within several hours. Several control experiments were performed without adding antibody or with anti-DNP IgE-coated cells preincubated with saturating levels of 2,4-DNP-glycine (Sigma).

Antigen-coated gels

Cross-linker synthesis

The *N*-succinimidyl ester of acrylamidohexanoic acid was synthesized in our laboratory as previously described (Pless et al., 1983). This bifunctional molecule was used to covalently couple the DNP ligand to polyacrylamide gel substrates as described below. In brief, the synthesis of this molecule involves two steps. In the first step, acryoyl chloride is reacted with 6-aminohexanoic acid under strongly basic conditions to form 6-acrylaminohexanoic acid. This intermediate is then reacted with *N*-hydroxysuccinimide and 1-ethyl-3-(3-dimethylaminopropyl) carbodiimide to form the bifunctional linker, *N*-succinimidyl acrylamidohexanoic acid. This product is purified via crystallization and stored at −20°C for later use in making polyacrylamide gel substrates.

Gel synthesis

Acrylamide, *N,N′*-methylene-bis-acrylamide, *N,N,N′,N′*-tetramethylethylene diamine (TEMED), and ammonium persulfate were from Bio-Rad Laboratories (Hercules, CA). Acrylamide (40%) (40 g monomer/100 ml) highly cross-linked (0.1 g cross-linker/g total monomer) gels were cast for 1 h, using 0.20-mm Teflon spacers in a vertical gel caster (SE 215; Hoeffer Scientific, San Francisco, CA). The monomer solution contained 54 mM HEPES buffered to pH 6.0. Initializers, 0.209 ml TEMED and 0.557 ml ammonium persulfate per 100 ml of monomer solution, were added. The monomer solution contained from 0.1 to 5 mM of bifunctional linker for copolymerization with acrylamide.

Covalent coupling of dinitrophenyl ligand

After casting, gels are removed from vertical caster and rinsed in ice-cold deionized water for 15 min. Linker molecules in half of the gel are then inactivated by immersion of the gel edgewise into 1.0 μl/ml ethanolamine in a buffer of 50 mM HEPES, 10% ethanol, in deionized water (pH 8.0) for

10 min. Derivatization of the gel with *N*-ϵ-2,4-DNP-lysine hydrochloride (Sigma) is as previously described (Tempelman and Hammer, 1994; Tempelman, 1993). Briefly, gels are placed in a saturated solution of *N*-ϵ-2,4-DNP-lysine hydrochloride for 2 h. Gels are then treated to cap unreacted linker active sites by a 30-min incubation in ethanolamine solution. Gels are then rinsed in ice-cold water and stored in water at 4°C for use within 2 weeks.

DNP surface density

Polyacrylamide gel DNP surface density was measured via base hydrolysis of the amide linkage as previously described (Tempelman, 1993; Tempelman and Hammer, 1994). Hydrolysis was performed on gel circles 1.1 cm in diameter and, on average, 140 μm thick (measured by optical sectioning). Circles were taken from different regions of the derivatized gel to assess DNP uniformity in the gel. Volumetric DNP density was converted to surface density, assuming all DNP molecules present in the top 1 nm of gel are accessible to cell surface IgE molecules. Table 2 provides the calculated DNP surface density for gel linker concentrations used in this study. The surface density of DNP in individual gels was found to be uniform (less than 3% variation).

Flow chamber and equipment

The flow chamber is a parallel-plate chamber with separate buffer inlet and outlet and cell injection ports and accommodations to hold thin polyacrylamide gel substrates. A schematic of the flow chamber is shown in Fig. 4. The flow chamber is constructed of an optically clear acrylic top section with an aluminum base in which a sealed glass plate is mounted for holding the gel substrate. The fluid flow channel above the gel is of dimensions 7.0 × 2.0 × 0.040 cm (L × W × H). These dimensions provide for an approximately linear shear field on the length scale of the cell. The height of the flow channel is defined by the thickness of the Silastic gasket (Dow Corning, Midland, MI) and is measured optically for each assembly. The top and lower pieces are held together with stainless bolts to form a leak-free seal. Buffer flow to the chamber is provided by a syringe pump (model 906; Harvard Apparatus, South Natick, MA) with a 500-ml syringe (Scientific Glass Engineering, Austin, TX). Volumetric flow rates are measured during each experiment.

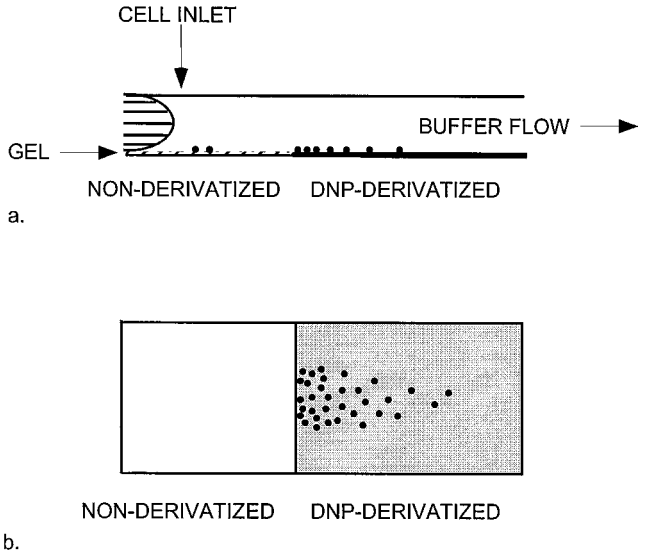

FIGURE 4 Side (*a*) and top (*b*) views of parallel-plate flow chamber. Nominal flow channel dimensions are 7 × 2 × 0.04 cm (L × W × H). IgE-sensitized cells are injected via cell inlet and allowed to settle through stationary buffer on a nonderivatized (DNP-free) portion of the gel substrate. Buffer flow is initiated, and cells are convected over and in contact with the DNP-derivatized portion of the gel substrate. Cell translational velocity is measured during perfusion via video microscopy. The population extent of adhesion and the cell spatial pattern are measured postflow via automated scanning video microscopy.

The flow chamber design allows for unobstructed microscopic viewing of the entire gel. The chamber assembly is mounted on a LUDL motorized *x-y* translation stage (LUDL Electronics Products, Hawthorne, NY) installed on a Nikon Diaphot 200 inverted-stage microscope with phase-contrast optics (Nikon, Melville, NY). Cells are observed at a final magnification of 125× while adherent cells are located, and at 315× while cell motion is tracked. The experiments are videotaped (Cohu CCD model 4915, Cohu, San Diego, CA; Sony VTR model SVO-9500 MD/2, Sony Corporation, New York, NY) for automated motion analysis. Data analysis and control of the videotape recorder and motorized stage is performed using LabVIEW and IMAQ Vision software (National Instruments, Austin, TX) with serial communication to a Pentium-based workstation. Images are imported to the workstation via an on-board capture card (model PCI-IMAQ 1408; National Instruments). Gels are automatically scanned for the number and location of adherent cells by software we developed for this application. Similar software tracks moving cells and reports their velocity and trajectory statistics.

Experimental method

The partially derivatized gel substrate is inserted into the flow chamber and the chamber is assembled. The flow channel gap height is measured by optical sectioning, and the flow width is measured by translating the motorized stage across the channel. Before the flow is initiated, cells (between 1000 and 2000) are injected onto the nonderivatized portion of the gel (Fig. 4). Cells are allowed to settle to the gel surface, and their location is scanned to record the number and location of injected cells. Flow of modified Tyrode's buffer is then initiated, and cell trajectories over several fields are videotaped for subsequent analysis. Cells enter and adhere to the region of the chamber coated with antigen. After nonadherent cells have cleared the chamber, the volumetric flow rate is measured. Buffer flow is then stopped. Because DNP is yellow, the location of the DNP interface can be clearly observed for high-DNP density gels. The interface in low-density (0.1 μmol/ml linker) gels is inferred from the cell binding pattern. The entire gel substrate is then scanned automatically by a computer algorithm, and the positions of all adherent cells are recorded. Injecting a mixture of air and buffer into the chamber at high velocity then clears adherent cells. A duplicate trial is then performed.

Shear rate determination

The buffer wall shear rate is calculated for all trials from the measured volumetric flow rate and daily measured chamber dimensions, $\gamma = 3Q/2Wd^2$, where γ is the wall shear rate in s^{-1}, Q is the volumetric flow rate in ml s^{-1}, W is the flow width in cm, and d is one-half the flow height in cm. Calibration studies with both 10.12- and 14.87-μm-diameter hard spheres (Coulter Corp., Hialeah, FL) indicated good agreement with theoretical predictions (Goldman et al., 1967a,b) for a bead-substrate separation distance of 5–20 nm (data not shown).

Cell counting and spatial coordinates

For each trial, the gel substrate is systematically scanned before and after buffer flow is initiated to record the number and position of all cells. This scan is performed on a predefined grid as follows: 1) The stage moves the objective into the first field of view (FOV). 2) The computer imports the current image and identifies all cells in the FOV based on preset criteria. 3) The center of area of each particle is updated to the current stage location. 4) The stage translates to the next FOV in the grid. In this manner, a nonoverlapping cell density map of the gel substrate is constructed. The scan time for the entire gel is ~20 min. Replicate scanning of several trial

cell adhesion patterns indicates ~2% error in the total number of adherent cells and a spatial resolution of less than one cell diameter.

Cell velocity

The translational velocity of nonadherent cells over the derivatized gel substrate is measured for each trial. The translation of cells in the lowest focal plane is videotaped. Cell velocity is measured from these video sequences by tracking the cells in a particular field of view over ~30 video frames. The velocity between frames is calculated by measuring the translation of the centroid from frame to frame (1/30th-s intervals). As in gel scanning, the centroid of each object is located via computer algorithms. The trajectory-average velocity for each cell is calculated. From this average for 4–20 cells, the trial population-average velocity is calculated.

Analysis

Percentage downstream adhesion

For each trial, the number of cells binding to the substrate in the DNP region is measured. From this, the percentage downstream adhesion (% adhesion) is calculated:

$$\text{percentage of adhesion} = 100^{*}T_b/(T_i - T_r) \qquad (1)$$

where T_b is the total number of cells bound past the DNP interface, T_i is the total number of cells injected at the cell inlet, and T_r is the number of cells remaining at the cell inlet after the trial. The term T_r accounts for the nonspecific adhesion of injected cells to the nonderivatized gel under static incubation before buffer flow. This term is generally less than 10% of T_i.

Adhesion rate constant

One can deduce the intrinsic rate constant for cell binding from the spatial pattern of adhesion using simple chemical kinetics. Note an advantage of this method is that all cells are in contact with the substrate at all times, thus eliminating macroscopic transport effects of cells being delivered normal to the substrate surface. Calibration studies performed with 20-μm polystyrene microspheres indicates a sphere-gel contact distance of 5–20 nm (data not shown). For each trial, the spatial binding pattern of cells adherent in the DNP-derivatized region of gel is fit to a first-order kinetic attachment model:

$$\frac{dN_b}{dt} = k_{ad}N_u = k_{ad}(N_{bf} - N_b(t))$$

$$\frac{dN_b}{dx} = \frac{k_{ad}}{\langle V\rangle}(N_{bf} - N_b(x))$$

which can be integrated to yield

$$\ln\left(1 - \frac{N_b(x)}{N_{bf}}\right) = -\frac{k_{ad}}{\langle V\rangle}x \qquad (2)$$

where N_u is the number of unbound cells at time t, N_b is the cumulative number of cells bound up to axial coordinate x (integrated across substrate width), N_{bf} is the total number of cells bound on the derivatized substrate after the experiment, $\langle V\rangle$ is the population average cell velocity for the trial over the derivatized region of gel, and k_{ad} is the adhesion rate constant. A plot of $-\ln(1 - N_b(x)/N_{bf})$ versus x has slope $k_{ad}/\langle V\rangle$. The adhesion rate constant concisely conveys the spatial binding pattern and provides a means of comparing the rates of cell-substrate binding as a function of experimental conditions.

Calculation of k_{ad} proceeds as follows (Figs. 5, 6, 7): 1) The experimental cell density map (Fig. 5) is integrated along the transverse coordinate for each axial coordinate x (Fig. 6). 2) The integrated data are plotted as $-\ln(1 - N_b(x)/N_{bf})$ versus the axial coordinate, as illustrated in Fig. 7. 3) A linear least-squares regression is performed on the initial linear region (before significant cell depletion). The slope of this regression is multiplied by $\langle V\rangle$ to obtain k_{ad}.

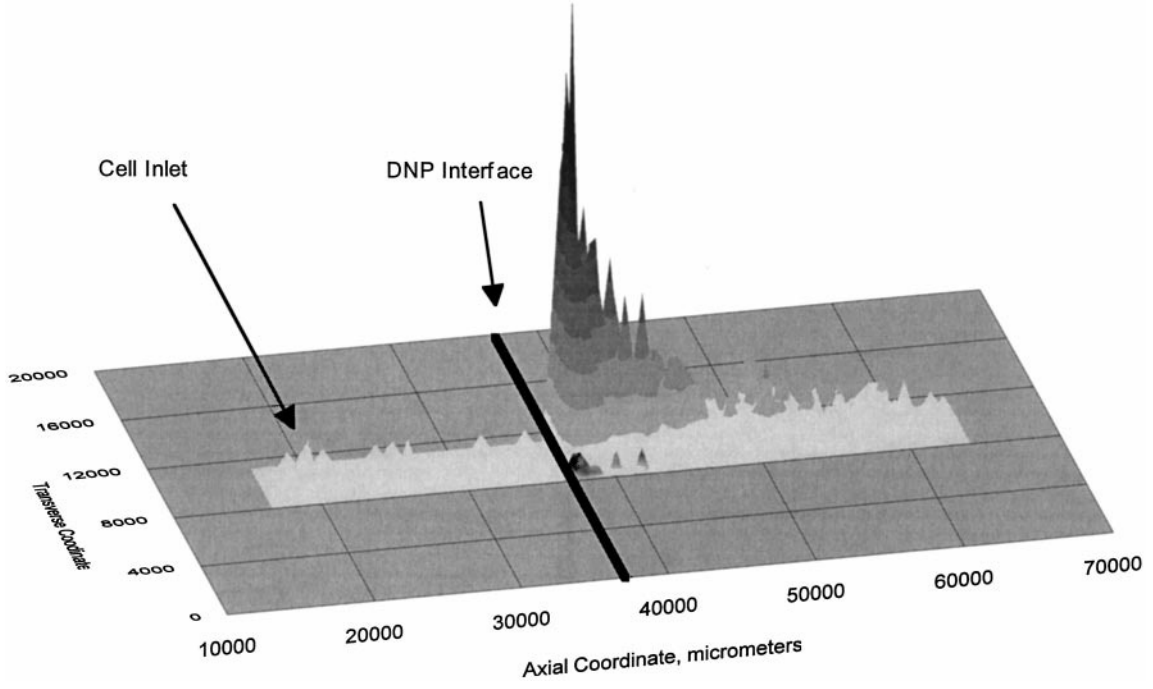

FIGURE 5 Spatial pattern of RBL cell adhesion in flow assay. Cells are injected into stationary buffer at the cell injection port and allowed to settle to the DNP-free portion of the substrate. Buffer flow sweeps the cells in the axial direction to the DNP interface and continues until all nonadherent cells exit the chamber at an axial coordinate of 7 cm. Conditions shown: SPE-7/DNP system, 52 s^{-1}, 1.3 $\times$ 10^4 anti-DNP sites per cell, 970 DNP/μm^2.

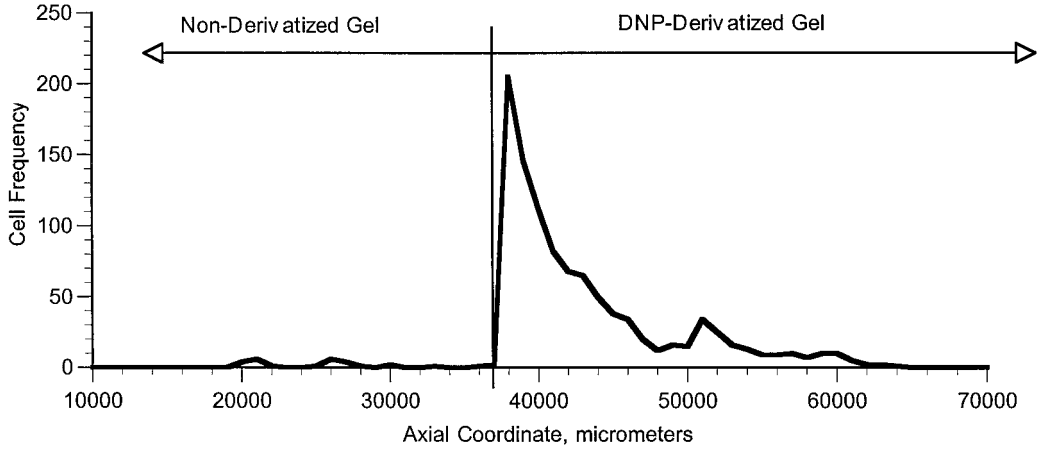

FIGURE 6 Cell binding as a function of axial position is obtained by integrating the cell density profile shown in Fig. 5 over the width of the chamber. The exponential decrease in cell frequency is fit to Eq. 2 for calculation of k_{ad}, as indicated in Materials and Methods.

RESULTS

Control experiments

Negative control experiments were performed to determine the level of nonspecific RBL cell adhesion to DNP-derivatized polyacrylamide gel substrates (DNP density of 1900 DNP/μm^2). Fig. 8 shows the results of these experiments. Binding over a range of wall shear rates was examined to determine whether any shear-dependent nonspecific adhesion was present in the system (possibly arising from the porosity of the gel). The data in series A represent the positive control in which cells were saturated with anti-DNP IgE. Untreated cells, cells treated with anti-dansyl IgE, and cells saturated with anti-DNP IgE and then blocked with DNP-glycine all show low levels of nonspecific adhesion. Furthermore, as seen in Fig. 5, a very low level of nonspecific adhesion occurs in the region of the gel that is not derivatized with DNP.

Dynamics of cell binding

In all attachment trials in this study with either IgE clone, only binary adhesion was observed between anti-DNP IgE-sensitized RBL cells and DNP-derivatized gel substrates. Cells either bound suddenly and irreversibly to the surface

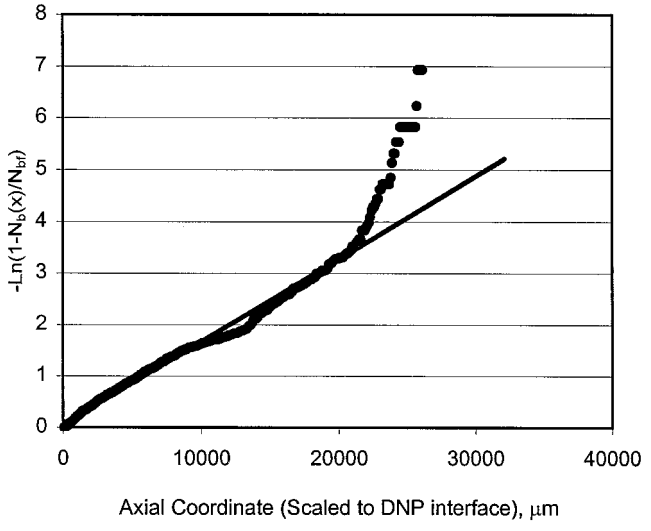

FIGURE 7 An illustration of the calculation of k_{ad}, using data from the flow experiment shown in Figs. 5 and 6. Linear regression of data at small axial coordinates (up to 0.5 cm) was used to calculate k_{ad} for the adhesion trial (see Materials and Methods). The figure illustrates a typical linear fit of the data. k_{ad} is proportional to the slope of the linear regression line as described by Eq. 2.

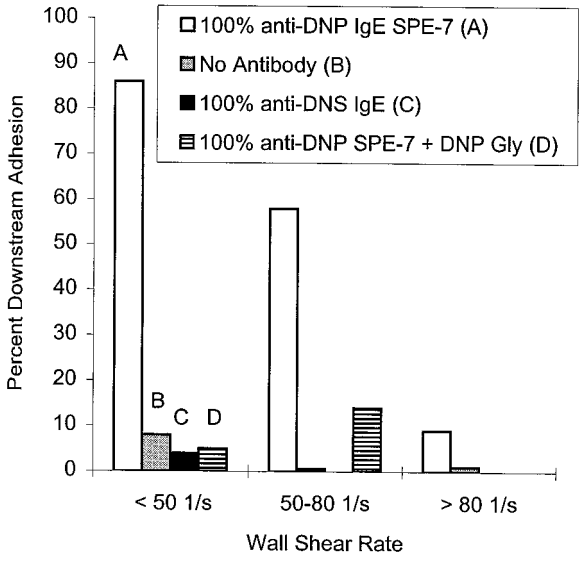

FIGURE 8 RBL cell adhesion in flow chamber assays: comparison of specific and nonspecific adhesion to DNP-ϵ-lysine derivatized gels. Cell treatments: (*A*) Cell saturation with anti-DNP. (*B*) Untreated cells. (*C*) Saturation with anti-dansyl IgE. (*D*) Cells coated with anti-DNP IgE, followed by blockage with free DNP-ϵ-glycine. The percent adhesion of a population of cells with the indicated surface treatment is shown for three ranges of wall shear rate. Nonspecific adhesion was less than 15% for all trials.

or continued at an unencumbered free-stream cell velocity. Occasionally, during attachment, a cell would arrest, translate one to two cell diameters, and then bind firmly. No significant cell detachment from the surface was observed in any trial.

Representative cell density maps for two attachment trials with SPE-7 are shown in Fig. 9. Conditions of IgE density, DNP density, and shear rate appear in the figure captions. We see that cell density is a maximum at an axial location just past the DNP interface and decreases with increasing distance from the interface. The extent of the decrease in cell density with distance varies with the experimental parameters (wall shear rate, receptor number, and ligand site density). The surface coverage of cells on the DNP gel in

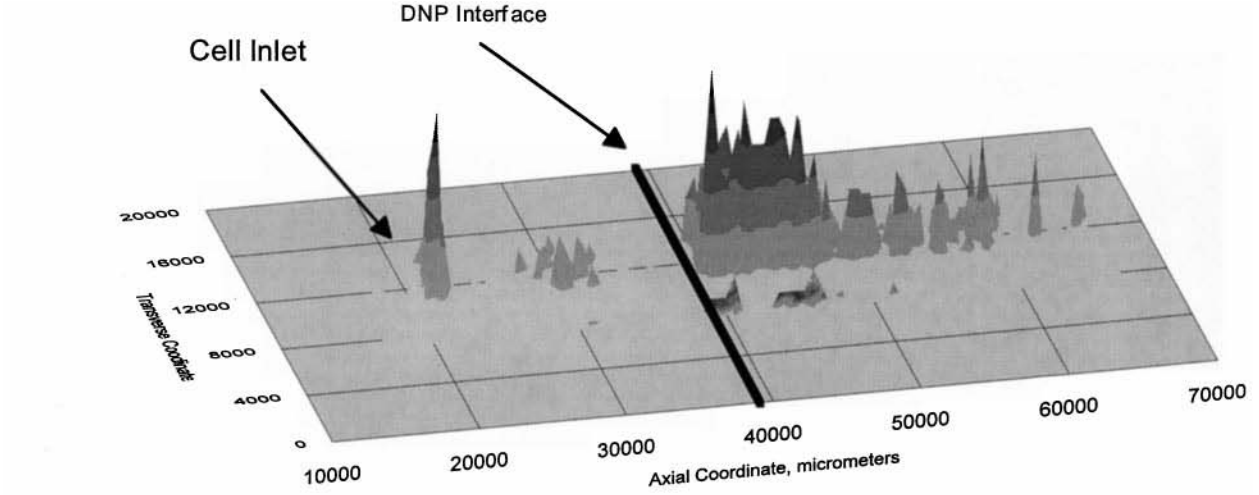

(a)

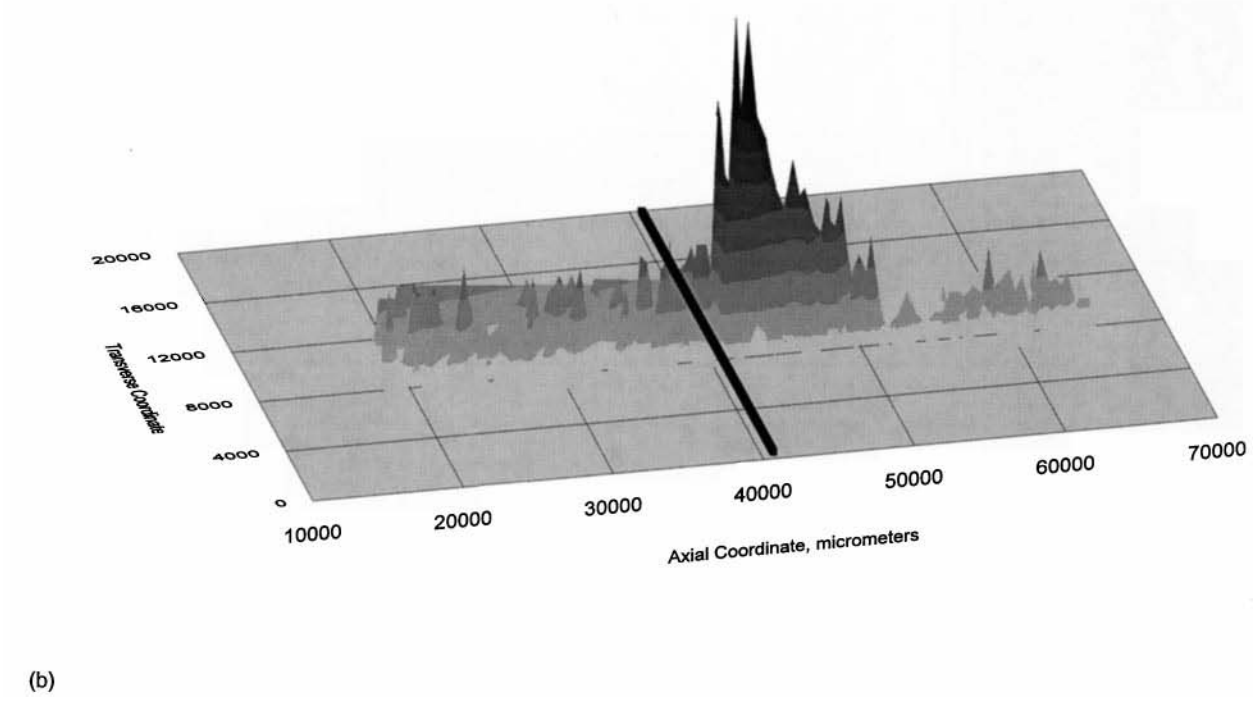

(b)

FIGURE 9 Examples of cell density maps from attachment experiments with the indicated wall shear rate, receptor number, DNP site density, percentage downstream adhesion, and k_{ad}. Flow is from left to right, with the cell injection port and DNP interface at the indicated axial coordinates. Conditions shown support approximately the same extent of adhesion, but the rate constant for adhesion is significantly different. (*a*) SPE-7/DNP system: 61 1/s, 1.3×10^4 anti-DNP sites per cell, 1900 DNP/μm^2, 76% adhesion, $k_{ad} = 0.025\ s^{-1}$. (*b*) SPE-7/DNP system: 35 1/s, 1.3×10^3 anti-DNP sites per cell, 1900 DNP/μm^2, 72% adhesion, $k_{ad} = 0.031\ s^{-1}$.

the region immediately past the interface generally was less than 10–15% of the total area; there was ample surface area for binding for all cells crossing the interface. Indeed, the number of cells fed to the chamber in each trial (~1500) was chosen to minimize cell-cell interactions at the interface while providing for statistically significant numbers of adherent cells (Fig. 14). This issue is addressed more thoroughly in the Discussion. It is also important to note that although the extent of adhesion is less than one, cell binding falls off significantly before the buffer outlet.

Extent of cell adhesion

Experiments were performed with the SPE-7/DNP receptor-ligand pair for different wall shear rates, SPE-7 site densities, and gel DNP surface density. A single series of attachment experiments were performed with the H1 26.82 anti-DNP clone for a single anti-DNP and DNP site density, at a full range of shear rates to allow for comparison to SPE-7 binding data. The extent of adhesion was measured for each experiment.

Fig. 10 shows the effect of shear rate on the percentage of adhesion for the SPE-7 clone for four combinations of cell receptor number and surface ligand density: (*A*) 13000 anti-DNP/cell, 1900 DNP molecules/μm^2; (*B*) 13,000 anti-DNP/cell, 280 DNP molecules/μm^2; (*C*) 13,000 anti-DNP/cell, 91 DNP molecules/μm^2; and (*D*) 1300 anti-DNP/cell, 1900 DNP molecules/μm^2. For comparison, data for the H1 26.82/DNP pair at 13,000 anti-DNP/cell, 1900 DNP molecules/μm^2 are also shown (*E*). Each point represents from one (no error bars) to five experiments at approximately the same wall shear rate. Vertical error bars represent the standard error in percentage adhesion between replicate trials. Horizontal error bars represent the standard error of the shear rate between replicates.

For both clones, and all receptor numbers and site densities, the percentage of adhesion to the DNP surface decreases with increasing wall shear rate within the error of the measurements. At low wall shear rate, adhesion is nearly complete when cell and substrate densities are high (*A* and *D*); decreases in receptor number or ligand density decrease the extent of adhesion at low shear rates (*B* and *C*). At high receptor number or ligand site densities, at a wall shear rate of 115 s^{-1}, percentage of adhesion decreases to the level of the negative control (*A* and *D*).

Fig. 10 also illustrates that receptor number and ligand site density influence the extent of adhesion. At 13,000 anti-DNP sites per cell, a decrease in DNP site density from 1900 μm^{-2} to 280 μm^{-2} decreases the extent of adhesion by approximately threefold. A further decrease in DNP density to 91 μm^{-2} results in a twofold reduction in adhesion at intermediate shear rates. Receptor number also influences the level of adhesion. A 10-fold decrease in receptor number decreases adhesion by 1.5-fold at intermediate shear. Thus decreases in site density or increases in shear rate lead to decreases in the extent of adhesion.

Effect of shear on the rate of adhesion

The spatial pattern of adhesion of SPE-7 or H1 26.82-coated RBL cells to DNP-derivatized gels was measured for the conditions shown in Fig. 10. Fig. 11 shows the k_{ad} values calculated from spatial patterns as described in Materials and Methods. Error bars represent the standard error in k_{ad} calculated for replicate trials. The shear rate dependence of k_{ad} for the H1 26.82/DNP pair was not measured previously

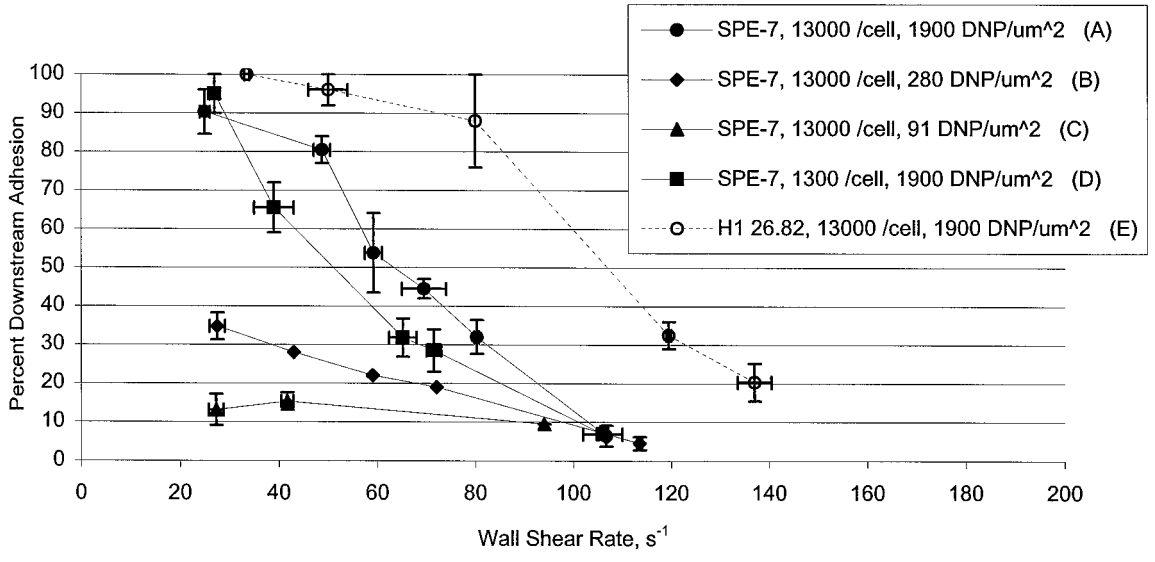

FIGURE 10 Shear rate dependence of the percentage RBL cell attachment in flow assays. Cells were sensitized with the indicated number of DNP binding sites. Polyacrylamide gels were derivatized with the indicated number of DNP molecules per unit area. Standard error bars indicate variability in measured percentage adhesion and wall shear rate between trials. Percentage adhesion decreases (within standard error) with increasing shear rate for all conditions shown.

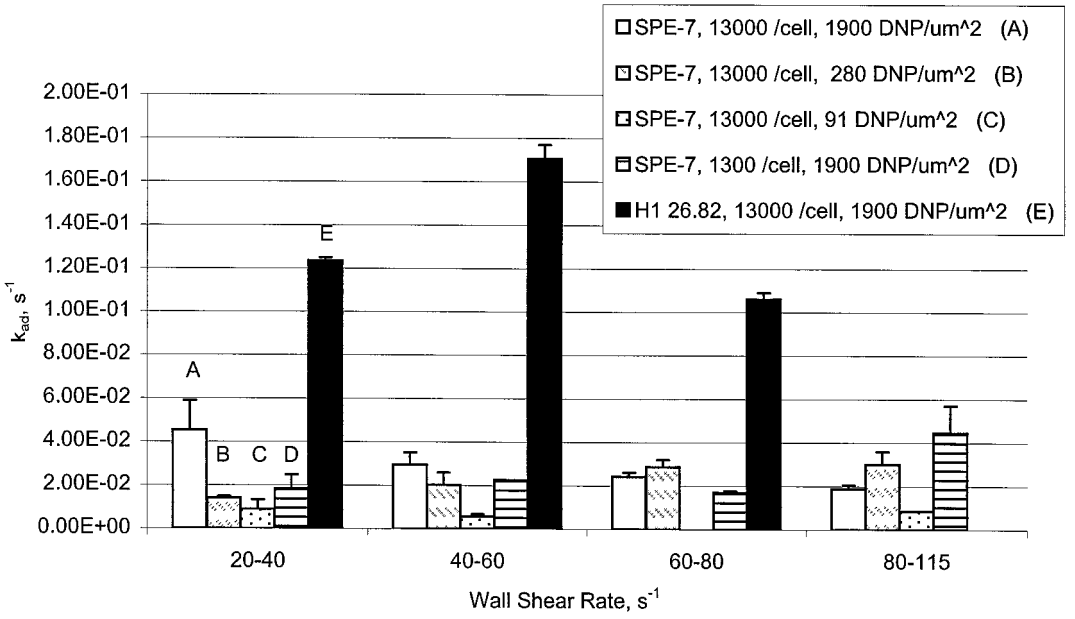

FIGURE 11 Overall adhesion rate constant as a function of wall shear rate in RBL cell attachment experiments. Cells were sensitized with the indicated number of DNP binding sites. Polyacrylamide gels were derivatized with the indicated number of DNP molecules per unit area. Error bars indicate the standard error in k_{ad}. The adhesion rate constant is a complex function of shear rate, increasing, decreasing, or remaining constant with increasing shear rate, depending on antibody number and DNP density.

by Tempelman and Hammer (1994) but has been examined for a limited set of DNP and H1 26.82 densities in this work. The letters A-E refer to conditions identical to those in Fig. 10. For the SPE-7 clone, the k_{ad} may increase or decrease with wall shear rate, depending on IgE or DNP density. At 13,000 receptors/cell and 1900 DNP/μm^2 (series A), k_{ad} decreases with shear rate from 20 to 115 s^{-1}. At a lower DNP density, 280 μm^{-2} (series B), k_{ad} increases with increasing shear. The positive correlation between k_{ad} and shear rate is maintained for 1300 IgE sites per cell and 1900 DNP/μm^2 (series D). Series C does not clearly support either a decreasing or increasing relationship between k_{ad} and wall shear rate.

Comparing series A, B, and C, we see that there is a strong dependence of k_{ad} on site DNP density. The nature of this relationship is also bimodal; at low shear rates k_{ad} decreases with decreasing DNP site density, but at high shear rates k_{ad} decreases or, within the error of the measurements, remains constant with increasing site density. This bimodal relationship is also seen in the relationship of k_{ad} to receptor number. At high DNP densities, k_{ad} decreases with decreasing receptor number at low shear, but increases or remains essentially constant with decreasing receptor number at high shear, within the error or the measurements. The result of these trends is that maxima in the rate constant for adhesion can occur at either high or low shear rate, depending on the density. Fig. 11 also illustrates that k_{ad} for the H1 26.82 is as much as sixfold greater than that for SPE-7 at identical conditions. The shear rate dependence for H1 26.82 is also bimodal; k_{ad} increases with shear at low shear rate, but decreases with shear rate as it is further increased.

Effect of receptor number on adhesion rate constant

Fig. 12 examines the dependence of k_{ad} on the number of anti-DNP binding sites per cell for SPE-7. Data in each series were collected at the indicated DNP site density and shear rate. All data were collected at a wall shear rate of ~50 s^{-1}, except for that at 91 DNP/μm^2, which was collected at 27 s^{-1}. This was done to have a statistically significant number of bound cells per trial for calculation of k_{ad}. In this figure, within the standard error of the measure-

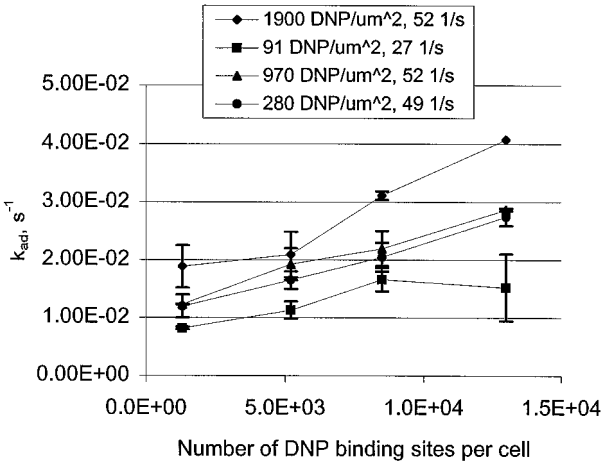

FIGURE 12 Overall adhesion rate constant as a function of the number of anti-DNP IgE (SPE-7) binding sites per cell. Gel DNP site densities and experimental wall shear rates are indicated for each series. Error bars indicate the standard error in k_{ad}. k_{ad} increases linearly with antibody number for all conditions shown (within the standard error).

ments, we observe a linearly increasing relationship between k_{ad} and the number of DNP binding sites per cell. The behavior does not appear at or near saturation. These curves do not extrapolate to zero at the low-density limit, possibly indicating a steep rise in k_{ad} at low receptor number.

Effect of antigen site density on adhesion rate constant

Fig. 13 examines the dependence of k_{ad} on DNP site density for adhesion with the SPE-7 clone. Data in each series are at the indicated fixed receptor number per cell and shear rate. k_{ad} increases with increasing DNP site density for all data series. The data at 8500, 5200, and 1300 receptors per cell are nearly overlapping over much of the range. Here, as in Fig. 12, the rate constant for adhesion increases with density nearly linearly over the entire range of DNP density. The dependence of k_{ad} on DNP density has not yet reached a plateau, and there appears to be a steep increase in k_{ad} with site density for less than 250 DNP/μm^2.

DISCUSSION

This paper provides results describing the attachment of anti-DNP IgE-sensitized RBL 2H3 cells to DNP-derivatized polyacrylamide gel substrates in a linear shear field. Two clones were used, SPE-7 and H1 26.82. Adhesion mediated by the H1 26.82 clone to DNP was measured previously for a limited number of conditions by Tempelman and Hammer (1994), but only the extent of adhesion was calculated in their study. We have better defined the shear-rate dependence of adhesion with this IgE clone and measured the rate constant of adhesion, k_{ad}, for the first time with this clone. These two model receptor-ligand pairs were chosen because both the chemical affinities and kinetic off rates are known or are measurable (SPE-7/DNP: $K_A = 4.8 \times 10^6\ M^{-1}$ and $k°_r = 0.19\ s^{-1}$ (first measured here); H1 26.82: $1.4 \times 10^8\ M^{-1}$ and $0.086\ s^{-1}$ (Erickson et al., 1986)), and because the SPE-7 clone has a lower on rate and affinity than H1 26.82 for the same antigen, DNP. As illustrated in Table 1, these molecular pairs represent a 30-fold difference in affinity and a 13-fold difference in on rate. With the SPE-7/DNP pair, we have systematically varied the wall shear rate, number of cell-bound anti-DNP binding sites, and gel DNP site density. In all trials, we have observed only binary adhesion of the cells to the substrates. The results indicate that the extent of cell adhesion decreases with increased wall shear rate, with decreased cell-surface anti-DNP binding site number, and with decreased gel substrate DNP site density. This paper also illustrates a method for determining the rate constant for adhesion, k_{ad}, from the spatial pattern of binding. This kinetic constant exhibits a complex dependence on shear rate, receptor number, and ligand density that has not previously been described. Unlike the extent of adhesion data, the adhesion rate constant is a single, robust, intrinsic parameter that quantifies the probability per unit time that a cell will bind and thus contains useful information that can be occluded by the extent of adhesion, which depends on assay geometry.

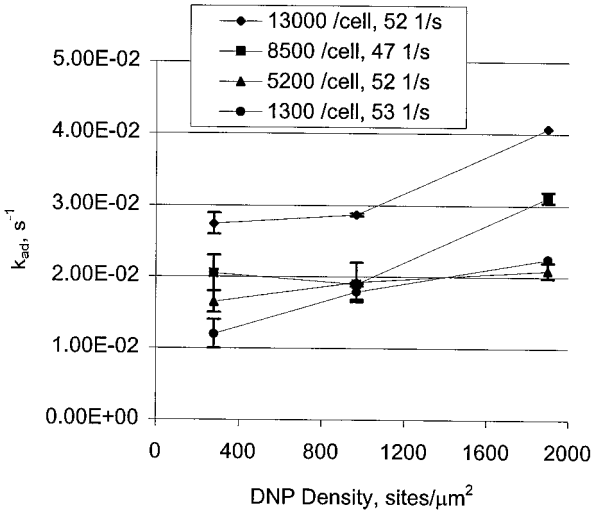

FIGURE 13 Overall adhesion rate constant as a function of gel DNP site density. Cell anti-DNP IgE (SPE-7) binding site density and experimental wall shear rate are indicated for each series. Error bars indicate the standard error in k_{ad}.

This paper is the first to report adhesion rate constants for the adhesion of cells to surfaces under hydrodynamic flow, using well-defined receptors and ligands. We have found that the binding of anti-DNP IgE-sensitized RBL cells to DNP-derivatized polyacrylamide gel substrates in a linear shear field is well represented by the first-order chemical rate equation (Eq. 2, Fig. 7). The representation is valid to the point where cell depletion becomes significant. We have examined the dependence of this rate constant on fluid wall shear rate, cell receptor number, and antigen site density. Furthermore, comparison of data from the SPE-7 and H1 26.82 clones gives information on k_{ad} about the importance of bond formation rate and affinity.

Ratio of receptor and ligand densities

Based on the reported microvilli length, 500 nm, and estimated IgE length, 150 nm (Tempelman, 1993), we assume only anti-DNP IgE molecules present on the tips of microvilli are available for binding to the planar adhesive substrate. Fc_ϵ receptors are known to be uniformly distributed over the entire RBL cell surface (Oliver et al., 1988). The total number of receptors accessible at the microvilli tips was previously calculated and found to be 6.5×10^3 Fc_ϵ receptors/cell (Tempelman and Hammer, 1994), so only a fraction of the total number of cell-bound IgE molecules are accessible to the surface. Therefore, the total number of IgE sites available to bind DNP ranges from 1.3×10^3 to 1.3×10^4/cell in this work. The ratio of ligand and receptor density is given in Table 2 for our experimental conditions. When the ligand density is reduced so that it is on the same order as the receptor density, adhesion is eliminated.

TABLE 1 IgE/antigen chemical affinities and solution reaction rates

Antigen (source)	IgE (source)	Affinity, K_A (M^{-1})	On rate, k_f ($M^{-1}\ s^{-1}$)	Off rate, k_r (s^{-1})	Reference
DNP-ϵ-lysine (Sigma)	SPE-7 (Sigma)	4.8×10^6	9.4×10^5	2.0×10^{-1}	This paper
DNP-ϵ-lysine (Sigma)	H1 26.82 (Dr. B. Baird, Cornell University)	1.4×10^8	1.2×10^7	8.6×10^{-2}	Erickson et al. (1986)

Binary binding behavior

The only dynamic state of adhesion seen in this work was firm arrest. Dynamic interactions previously described as transient adhesion (Chen et al., 1997; Hammer and Apte, 1992) or cell rolling (Brunk et al., 1996; Lawrence and Springer, 1993) were not observed with either of these anti-DNP IgE clones on DNP. We did not observe any significant release of cells from the substrate after initial attachment. This type of adhesion is similar to that reported with H1 26.82 on DNP by Tempelman and Hammer (Tempelman, 1993; Tempelman and Hammer, 1994). In their study, the extent of adhesion with the clone H1 26.82 was reported for the same DNP-polyacrylamide gel system as employed here, but for a limited number of shear rates. They did not quantify the rate constant of adhesion. They observed only firm adhesion with the H1 26.82 clone for a variety of conditions of site density and shear rate, consistent with the current results. Despite the approximately twofold higher solution off rate of SPE-7 than H1 26.82 to DNP, we did not observe any transient binding or detachment. This failure to support rolling comes despite an off rate of 0.19 s^{-1}, close to the 1 s^{-1} off rate between P-selectin and its ligand, PSGL-1 (Alon et al., 1995). The fact that P-selectin gives rolling and IgE/hapten interactions give firm adhesion likely reflects a fundamental difference in antibody-antigen interactions compared to selectin interactions (Brunk et al., 1996; Dore et al., 1993; Ley et al., 1993) or the possibility that an off rate of 0.19 s^{-1} is insufficient to support rolling.

TABLE 2 Ratio of DNP (ligand) to IgE (receptor) densities

Linker concentration (μmol linker/ml)	Gel DNP surface density (#/μm^2)	% anti-DNP IgE	Ligand density/ Receptor density
0.1	90	10	40
		40	9
		65	6
		100	4
1.0	280	10	110
		40	28
		65	18
		100	11
2.5	970	10	400
		40	100
		65	61
		100	40
5.0	1900	10	780
		40	200
		65	120
		100	78

Chang and Hammer have proposed a generalized phase diagram that predicts the dynamic state of cell-substrate adhesion based on the kinetic rate of receptor-ligand bond breakage (k_r) and on the bond's response to strain, represented by the Bell parameter γ (Bell, 1978; Chang, 1997). In light of the phase diagram predictions, we believe that although k_r is an appropriate value to permit rolling, γ for SPE-7/DNP interactions is outside of the range required to support dynamic bond formation and breakage rates under stress, regardless of the off rate (Alon et al., 1995; Chang, 1997). However, recent studies have shown that leukocytes can exhibit transient adhesion and unstable rolling interactions on IgM antibodies directed against carbohydrate antigens similar to the ligands for selectin molecules (Chen et al., 1997), so it may be that there are differences among antigen-antibody pairs in their response to stress. Accurate measurement of the Bell parameter for anti-DNP IgE/DNP interactions is required to predict the possibility of dynamic interactions with this system and to determine the validity of the phase diagram.

Extent of adhesion

The extent of anti-DNP IgE RBL cell adhesion to DNP-derivatized gel substrates shows a strong dependence on wall shear rate for both the SPE-7 and H1 26.82 clones (Fig. 10). The extent of adhesion decreases with shear rate from nearly complete adhesion to levels indistinguishable from negative control. Fig. 10 also shows the dependence of extent of adhesion on receptor number and ligand site density; extent decreases for decreases in both parameters. These trends were seen previously with the H1 26.82-coated RBL cells on DNP surfaces (Tempelman and Hammer, 1994). With SPE-7, a 10-fold reduction in receptor number decreases the extent of adhesion only slightly, whereas Tempelman and Hammer observed a nearly fivefold reduction with a fivefold reduction in H1 26.82 receptor number.

As an additional control, we have investigated whether cell-cell interactions affect the extent and rate of cell binding. In most of the experiments shown here, ~1500 cells were injected into the chamber, and this led to at most a 15% cell coverage of the gel in the area immediately near the interface. This number is much smaller than is typically used in a cell adhesion experiment and is designed to be sufficiently small to minimize cell-cell interactions while keeping the errors of measurement modest. To assess whether this extent of coverage leads to cell-cell collisions and thus affects our measurement of adhesion rate con-

stants, we have examined the percentage of adhesion and k_{ad} obtained for a range of numbers of cells injected. Fig. 14 illustrates this data for two shear rate values: (*a*) 50 s^{-1} and (*b*) 80 s^{-1}. The antibody number in all cases was 1.3 $\times$ 10^4/cell, and DNP density was 1900 DNP/μm^2, conditions that led to maximum binding for the SPE-7 IgE. In Fig. 14, *a* and *b*, within the error of the measurements, the percentage of adhesion and k_{ad} appear to be independent of the

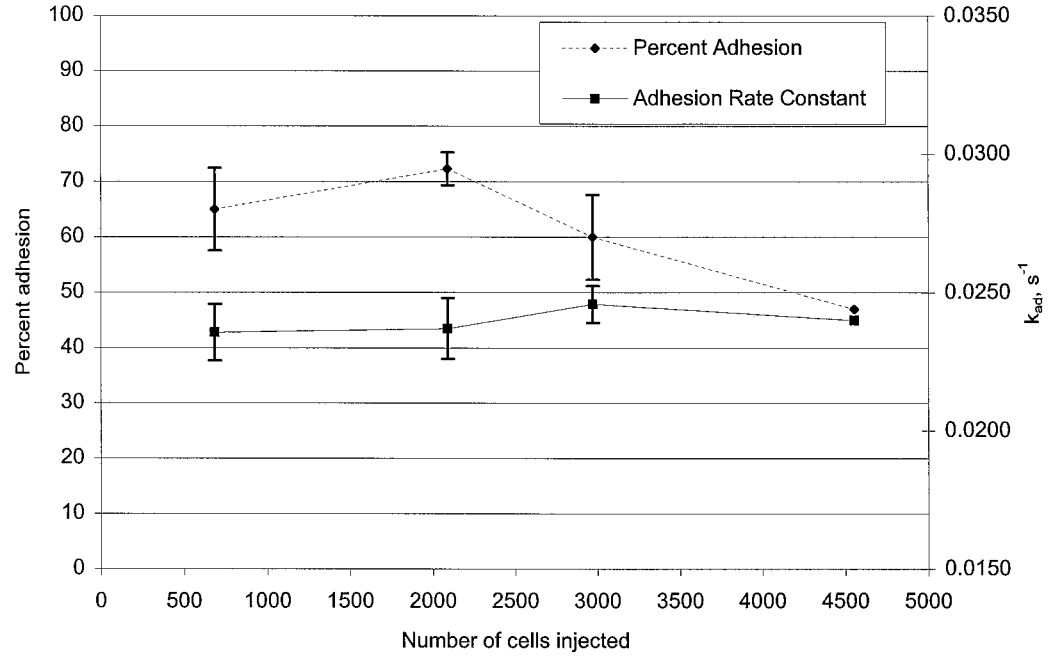

a.

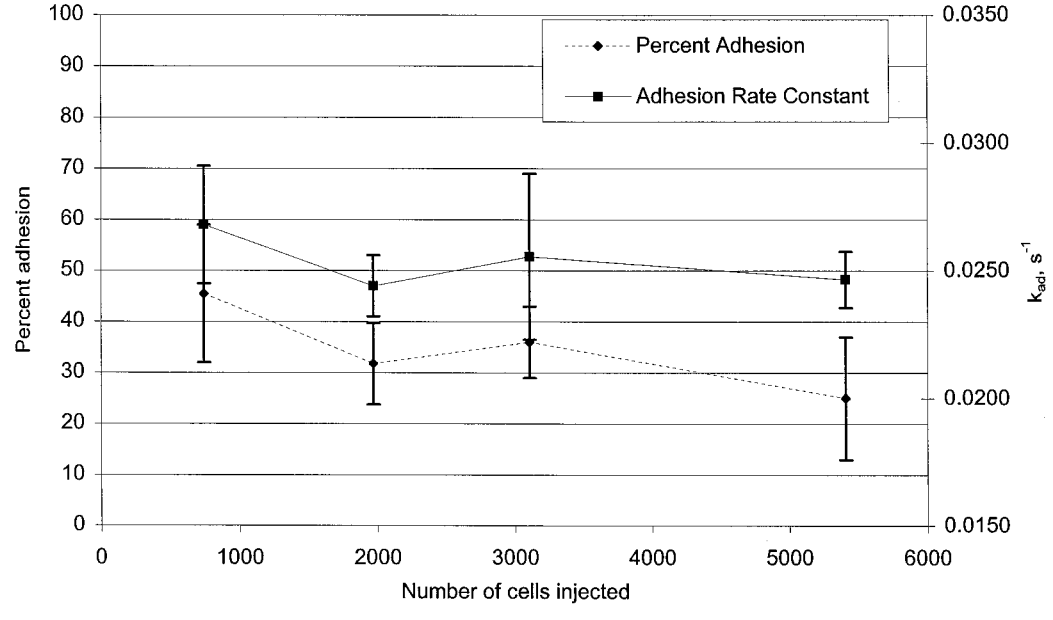

b.

FIGURE 14 Effect of varying the feed cell number on measured percentage adhesion and k_{ad}. The DNP site density was 1900 DNP/μm^2, and the antibody number was 1.3 $\times$ 10^4/cell in all trials. *a* indicates that both the percentage adhesion and k_{ad} are independent of cell number below 2000 cells for a wall shear rate of 50 s^{-1}. *b* indicates that percentage adhesion and k_{ad} are independent of cell number below 2000 at a wall shear rate of 90 s^{-1}. Error bars indicate the standard error of the measurements ($2 > n > 5$). Adhesion does not appear to be sensitive to the number of injected cells at the numbers employed in these flow experiments (~1500 per trial).

number of cells injected into the chamber. This indicates that at these cell numbers, the binding is not significantly affected by cell-cell interactions. Any reduction in cell number beyond the smallest number used here (750) would result in greater errors (a larger noise-to-signal ratio). Although an area coverage of 15% might appear to be sufficiently high to induce cell-cell interactions, the coverage occurs only in a small region of the gel, which explains why the adhesion is independent of cell density. Thus we believe we are measuring the intrinsic rate constant of cell-substrate binding independently of cell density effects.

We observed that the range over which the extent of adhesion is shear-sensitive is significantly different for the two clones. Adhesion is significant with clone H1 26.82 to beyond 140 s^{-1}, whereas with clone SPE-7 adhesion drops off to negative control levels near 100 s^{-1}. Comparing the kinetic rates for these clones, H1 26.82 has a 13-fold higher solution on rate than SPE-7. Thus it appears that a larger value of on rate can lead to a significant increase in the shear rates that can support adhesion. Furthermore, at certain intermediate shear rates, the higher on rate for H1 26.82/DNP yields a significantly higher extent of binding than the slower reacting SPE-7/DNP pair. Thus, depending on the shear rate, there can be a significant affect of on rate on binding.

Fig. 10 illustrates a clear dependence of extent of adhesion on both receptor number and antigen site density. According to the ratios of antigen to IgE density given in Table 2, antigen molecules should be in excess. In this regime, we would expect only a weak dependence of adhesion on DNP density, but a strong dependence on receptor number, so the observed sensitivity of adhesion to DNP density is somewhat surprising. The extent of adhesion does not appear to be limited by the transport of receptors to ligand molecules because, as seen in Figs. 5 and 9, nearly all cells that bind do so shortly after reaching the DNP interface; there are only low levels of adhesion near the chamber exit. An alternative explanation for the strong ligand density dependence may come from overestimating ligand density. In these calculations, DNP molecules in the top 1 nm of the porous gel are assumed to be accessible to passing anti-DNP binding sites. The actual density of accessible DNP molecules in the gel may be significantly less than the estimates in Table 2 and thus affect our interpretation of these data.

It is important to note that the percentage of cells adhering in the flow assay is not a unique measure of adhesiveness. Fig. 9 illustrates the spatial pattern of adhesion for two trials in which approximately the same percentage of adhesion was observed. However, the pattern and the rate of adhesion are significantly different in these trials. This fundamental difference in adhesiveness is indicated by the ~25% larger adhesion rate constant for the trial in Fig. 9 *b*. It is also interesting to note that the rate constant for attachment does not necessarily decrease with shear, but can actually increase, as was pointed out in recent simulations (Chang, 1997; Chang and Hammer, manuscript submitted for publication). In Figs. 10 and 11, the extent always decreases with increasing shear, but k_{ad} may increase, remain approximately constant, or decrease. These examples illustrate the importance of using the adhesion rate constant, rather than the extent of adhesion, to characterize attachment in flow assays.

Adhesion rate constant

As shown in Fig. 11, the dependence of the adhesion rate constant on wall shear rate for SPE-7 depends on the values of receptor and ligand site densities. The complex relationship between binding rate and shear rate is further demonstrated by data for the H1 26.82 clone. These data indicate a bimodal dependence of k_{ad} on shear rate and site density and illustrate that this rate constant is generally more sensitive to experimental conditions than the extent of adhesion; hence it is a more sensitive metric of adhesion.

Chang has modeled the rate of binding of cell-bound receptors to surface-immobilized ligands under flow (Chang, 1997; Chang and Hammer, manuscript submitted for publication). In their model system, cells are treated as receptor-coated hard spheres translating over a ligand-coated substrate in a shear field. The two-dimensional convection-diffusion equation is solved to obtain the receptor-ligand encounter rate, based on the relative velocity of the reactive species. A Peclet number is used to define the relative importance of receptor convection versus diffusion in the cell-substrate contact area. The Peclet number, Pe, is defined by Pe = (radius of Fc_ϵ receptor)(cell slip velocity)/(Fc_ϵ receptor diffusivity). Thus the Peclet number is proportional to the cell slip velocity, which scales with the shear rate (Goldman et al., 1967a,b). The probability that an encounter will lead to bond formation depends on the intrinsic on rate and on the receptor-ligand contact duration. The adhesion rate constant is the product of the encounter rate and the reaction probability. The encounter rate increases with relative velocity (Pe), whereas the contact duration decreases. Thus k_{ad} represents a conflict between the frequency of encounter versus the duration. This theory predicts that k_{ad} increases linearly with the product of receptor and ligand site densities and increases in a complex manner with Peclet number and intrinsic on rate. In a transport-limited regime, k_{ad} is a strongly increasing function of cell velocity. As the relative velocity increases, binding becomes reaction-limited, and k_{ad} reaches a plateau determined by the intrinsic on rate. In no instance in their model does k_{ad} decrease with increasing relative velocity.

To compare our data with this model, the Peclet number for each experimental trial was calculated based on the estimated RBL slip velocity at each shear rate (Goldman et al., 1967a,b) and on values of receptor radius (10^{-7} cm) and receptor diffusivity (2×10^{-10} cm^2/s) (Tempelman and Hammer, 1994). The Peclet number in all trials was greater than 1, indicating that binding is dominated by convective motion of the cell, not diffusion in the contact region. Based on estimates of the intrinsic on rate for SPE-7 and H1 26.82

(10^8 s^{-1} and 10^9 s^{-1}; Bell, 1978), this theory predicts transport limitation for most experiments performed in this study, with others being neutral or slightly reaction limited.

The bimodal dependence of k_{ad} on Pe (shear rate) in Fig. 11 appears consistent with a transition from the transport limit (low shear rate) to reaction limit (high shear rate). In the transport-limited regime, cells would translate until a collision occurred and a bond was formed. Increasing cell velocity (Pe) would increase the frequency of encounter and thus the transport-limited binding rate. This enhancement of binding with shear rate is similar to the shear threshold requirement for adhesion seen with L-selectin-mediated binding (Finger et al., 1996). It appears that a high rate of collision promotes adhesion in this regime with these systems. In a reaction-limited regime, the duration of an average receptor-antigen contact is less than the time required for the molecular rearrangements to occur for the formation of a bond. Increasing cell velocity in the reaction-limited regime would decrease the contact duration, decreasing the binding rate. Thus one consistent explanation for the increase and then decrease in k_{ad} with shear rate is a crossover from the transport to a reaction-limited regime.

The dependence of k_{ad} on site density also appears to be bimodal. At low to intermediate shear rate, k_{ad} increases approximately linearly with site density (Figs. 11, 12, and 13), in agreement with the theory. At high shear rate, however, k_{ad} appears to remain constant with increasing site density. The increase at low shear appears intuitively correct; increasing the frequency of encounter for fixed contact duration should increase the rate of binding. The behavior at high shear is not the same as that at low shear. Referring back to our discussion of transport effects, it is possible that high shear provides for a sufficiently fast encounter that can overcome any deficiencies in ligand density.

Data for the H1 26.82 clone in Fig. 11 also show an increase in k_{ad} with shear rate at low shear, followed by a decrease at high shear. This may indicate that we have moved from transport to reaction-limited regimes by varying only the shear rate. The maxima in these data would indicate a point of balance between transport and reaction-limited effects. The magnitude of k_{ad} for H1 26.82 is much greater than that for SPE-7 attachment at the same conditions (Fig. 11, series *E* versus *A*). We believe that this difference is due solely to a difference in on rate. It is widely believed that attachment is governed by on rate (Tempelman and Hammer, 1994; Hammer and Apte, 1992). The model of Chang and Hammer supports this hypothesis. The H1 26.82/DNP-ϵ-lys solution on rate is ~13-fold greater than that of SPE-7. As shown in Fig. 11, this difference leads to as much as a 5.5-fold difference in k_{ad} and significant differences in extent of adhesion.

Effect of cell heterogeneity

The number of RBL cell surface Fc_ϵ receptors is known to vary with the cell cycle. Cells used in these flow assays are not synchronized in the cell cycle and should therefore possess a distribution of anti-DNP binding sites when sensitized with IgE. Receptor numbers given in this paper represent the mean value. We did not measure the density of IgE receptors on these cells, but Ryan (1989) reported they were log-normally distributed. The distribution around this mean is not known for the cells used in these trials. It is clear that cell heterogeneity will have an impact on the adhesion extent and rate of a cell population.

A remarkable feature of the data in Fig. 10 is the broad range of shear rates over which percentage of adhesion decreases from complete to nearly no adhesion. We view percentage of adhesion in these experiments as the fraction of cells in the population that possess a sufficient number of receptors to bind the surface for the shear rate of interest. It is clear from the data in Figs. 9 and 10 that at moderate to high shear rates, only a fraction of cells bind. We postulate that heterogeneity in individual cell receptor number leads to incomplete adhesion at all but the highest shear rates, where we reach the reaction limit. As shear increases in Fig. 10, fewer cells have sufficient receptors to bind and the extent of adhesion diminishes. From the spatial pattern in Fig. 9, the majority of cells that bind at elevated shear do so far from the end of the chamber; cells with sufficient receptor number do have adequate time to form bonds. With this, cell heterogeneity appears to be an important factor in determining percentage of adhesion.

As with the extent of adhesion, we believe that k_{ad} values reflect, to some extent, heterogeneity. As illustrated in Fig. 7, k_{ad} is determined by examining the bound cell density in the asymptotic region nearest the beginning of the antigen-binding domain. Far from this domain, binding falls off, and this may represent slower binding mediated by cells with lower receptor density. In Fig. 12, we have seen that k_{ad} is sensitive to receptor number. The measured k_{ad} will reflect the binding rate of cells with the mean number as well as those with a greater number or less than the mean number. For a symmetrical distribution of receptor number and nearly complete adhesion, the measured k_{ad} should be only weakly influenced by receptor number heterogeneity. However, when we calculate k_{ad} for trials with incomplete adhesion, we likely obtain a value corresponding to a mean receptor number greater than that of the population injected into the chamber.

Future studies of the rate and extent of adhesion should investigate the role of cell heterogeneity by purifying cells of a particular receptor number and measuring k_{ad} and percentage of adhesion in similar flow assays. By comparison to the adhesive behavior of the entire population, we may more clearly understand the role of receptor number heterogeneity in attachment phenomena.

This work was supported by the National Science Foundation (BES-9796090) and the National Institutes of Health (AI 35997). We are grateful to Barbara Baird and Dave Holowka for the gift of the H1 26.82 IgE monoclonal antibody.

REFERENCES

Alon, R., D. A. Hammer, and T. A. Springer. 1995. Lifetime of the P-selectin-carbohydrate bond and its response to tensile force in hydrodynamic flow. *Nature.* 374:539–542.

Atherton, A., and G. V. R. Born. 1972. Quantitative investigations of the adhesiveness of circulating polymorphonuclear leukocytes to blood vessel walls. *J. Physiol. (Lond.).* 222:447–474.

Barsumian, E. L., C. Isersky, M. G. Petrino, and R. P. Siraganian. 1981. IgE-induced histamine response from rat basophilic leukemia cell lines: isolation of releasing and nonreleasing clones. *Eur. J. Immunol.* 11: 317–323.

Bell, G. I. 1978. Models for the specific adhesion of cells to cells. *Science.* 200:618–627.

Bongrand, P., and G. I. Bell. 1984. Cell-cell adhesion: parameters and possible mechanisms. *In* Cell Surface Dynamics: Concepts and Models. Marcel Dekker, New York. 459–493.

Brunk, D. K., D. J. Goetz, and D. A. Hammer. 1996. Sialyl Lewis x/E-selectin-mediated rolling in a cell-free system. *Biophys. J.* 71: 2902–2907.

Brunk, D. K., and D. A. Hammer. 1997. Quantifying rolling adhesion with a cell-free assay: E-selectin and its carbohydrate ligands. *Biophys. J.* 72:2820–2833.

Chang, K.-C. 1997. Adhesive dynamics simulation of receptor-mediated cell adhesion on surfaces under flow. Ph.D. thesis. School of Chemical Engineering, Cornell University.

Chen, S., R. Alon, R. C. Fuhlbrigge, and T. A. Springer. 1997. Rolling and transient tethering of leukocytes on antibodies reveals specialization of selectins. *Proc. Natl. Acad. Sci. USA*. 94:3172–3177.

Dore, M., R. J. Korthuis, N. Granger, M. L. Entman, and C. W. Smith. 1993. P-selectin mediates spontaneous leukocyte rolling in vivo. *Blood.* 82:1308–1316.

Erickson, J., B. Goldstein, D. Holowka, and B. Baird. 1987. The effect of receptor density on the forward rate constant for binding of ligands to cell surface receptors. *Biophys. J.* 52:657–662.

Erickson, J., P. Kane, B. Goldstein, D. Holowka, and B. Baird. 1986. Cross-linking of IgE-receptor complexes at the cell surface: a fluorescence method for studying the binding of monovalent and bivalent haptens to IgE. *Mol. Immunol.* 23:769–781.

Erickson, J. W., R. G. Posner, B. Goldstein, D. Holowka, and B. Baird. 1991. Bivalent ligand dissociation kinetics from receptor-bound IgE: evidence for a time-dependent increase in ligand rebinding at the cells surface. *Biochemistry.* 30:2357–2363.

Finger, E. B., K. D. Puri, R. Alon, M. B. Lawrence, U. H. von Andrian, and T. A. Springer. 1996. Adhesion through L-selecting requires a threshold hydrodynamic shear. *Nature*. 379:266–269.

Goldman, A. J., R. G. Cox, and H. Brenner. 1967a. Slow motion of a sphere parallel to a plane wall. I. Motion through a quiescent fluid. *Chem. Eng. Sci.* 22:637–651.

Goldman, A. J., R. G. Cox, and H. Brenner. 1967b. Slow motion of a sphere parallel to a plane wall. II. Motion through a quiescent fluid. *Chem. Eng. Sci.* 22:653–660.

Goldstein, B., R. Posner, D. Torney, J. Erickson, D. Holowka, and B. Baird. 1989. Competition between solution and cell surface receptors for ligand. *Biophys. J.* 56:100–108.

Hammer, D. A., and S. M. Apte. 1992. Simulation of cell rolling and adhesion on surfaces in shear flow: general results and analysis of selectin-mediated neutrophil adhesion. *Biophys. J.* 63:35–57.

Kansas, G. S. 1996. Selectins and their ligands: current concepts and controversies. *Blood.* 88:3259–3287.

Lawrence, M. B., and T. A. Springer. 1993. Neutrophils roll on E- selectin. *J. Immunol.* 151:6338–6346.

Ley, K., T. F. Tedder, and G. S. Kansas. 1993. L-selectin can mediate leukocyte rolling in untreated mesenteric venules in vivo independent of E- or P-selectin. *Blood.* 82:1632–1638.

Metzger, H., G. Alcaraz, R. Hohman, J. Kinet, V. Pribluda, and R. Quarto. 1986. The receptor with high affinity for immunoglobulin E. *Annu. Rev. Immunol.* 4:419–70.

Oliver, J. M., J. Seagrave, R. F. Stump, J. R. Pfeiffer, and G. G. Deanin. 1988. Signal transduction and cellular response in RBL-2H3 mast cells. *Prog. Allergy.* 42:185–245.

Pauli, B. U., H. G. Augustin-Voss, M. E. El-Sabban, R. C. Johnson, and D. A. Hammer. 1990. Organ-preference of metastasis. *Cancer Metastasis Rev.* 9:175–189.

Pless, D. D., Y. C. Lee, S. Roseman, and R. Schnaar. 1983. Specific cell adhesion to immobilized glycoproteins demonstrated using new reagents for protein and glycoprotein immobilization. *J. Biol. Chem.* 258: 2340–2349.

Ryan, T. A. 1989. Signal transduction of immunoglobulin E receptor cross-linking. Ph.D. thesis. Cornell University.

Springer, T. A. 1990. Adhesion receptors of the immune system. *Nature.* 346:425–434.

Taurog, J. D., C. Fewtrell, and E. L. Becker. 1979. IgE mediated triggering of rat basophilic leukemia cells: lack of evidence for serine esterase activation. *J. Immunol.* 122:2150–2153.

Tempelman, L. A. 1993. Quantifying receptor-mediated cell adhesion under fluid flow using a model granulocyte cell line. Ph.D. thesis. School of Chemical Engineering, Cornell University.

Tempelman, L. A., and D. A. Hammer. 1994. Receptor-mediated binding of IgE-sensitized rat basophilic leukemia cells to antigen-coated substrates under hydrodynamic flow. *Biophys. J.* 66:1231–1243.

Weetal, M. 1992. Studies on the high affinity receptor for IgE (FceRI): binding of chimeric IgE/IgG and desensitization of cellular responses. Thesis. Department of Chemistry, Cornell University.